

Highly Efficient Fumed Silica Nanoparticles for Peptide Bond Formation: Converting Alanine to Alanine Anhydride

Chengchen Guo,^{*,†} Jacob S. Jordan,[†] Jeffery L. Yarger,^{†,‡} and Gregory P. Holland^{*,‡}

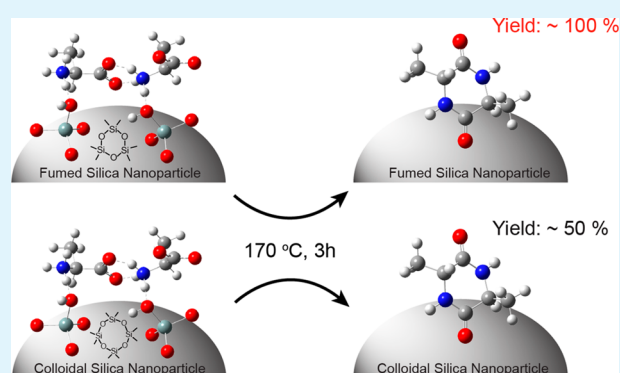
[†]School of Molecular Sciences, Magnetic Resonance Research Center, Arizona State University, Tempe, Arizona 85287-1604, United States

[‡]Department of Chemistry and Biochemistry, San Diego State University, 5500 Campanile Drive, San Diego, California 92182-1030, United States

S Supporting Information

ABSTRACT: In this work, thermal condensation of alanine adsorbed on fumed silica nanoparticles is investigated using thermal analysis and multiple spectroscopic techniques, including infrared (IR), Raman, and nuclear magnetic resonance (NMR) spectroscopies. Thermal analysis shows that adsorbed alanine can undergo thermal condensation, forming peptide bonds within a short time period and at a lower temperature (~ 170 °C) on fumed silica nanoparticle surfaces than that in bulk (~ 210 °C). Spectroscopic results further show that alanine is converted to alanine anhydride with a yield of 98.8% during thermal condensation. After comparing peptide formation on solution-derived colloidal silica nanoparticles, it is found that fumed silica nanoparticles show much better efficiency and selectivity than solution-derived colloidal silica nanoparticles for synthesizing alanine anhydride. Furthermore, Raman spectroscopy provides evidence that the high efficiency for fumed silica nanoparticles is likely related to their unique surface features: the intrinsic high population of strained ring structures present at the surface. This work indicates the great potential of fumed silica nanoparticles in synthesizing peptides with high efficiency and selectivity.

KEYWORDS: fumed silica nanoparticles, alanine, alanine anhydride, adsorption, thermal transformation, NMR spectroscopy, Raman spectroscopy



INTRODUCTION

The adsorption and transformation of biomolecules on surfaces of inorganic materials have attracted considerable attention in recent years since it is of major significance in prebiotic chemistry, bio-nanotechnology, and drug delivery research.^{1–8} A number of studies in recent decades have demonstrated that formation of peptide bonds at relatively low temperatures in the absence of any activating agents can be realized when gently heating amino acids adsorbed at the interfaces of inorganic oxides such as silica, alumina, or minerals.^{9–13} There has been considerable interest in solving: “the origin of the first peptide” in prebiotic chemistry, with some recent studies illustrating that mineral surfaces might have served as catalysts for peptide bond formation, making possible the synthesis of the first small oligopeptides.¹⁴ The surface-catalyzed peptide bond formation reaction is of particular interest in synthetic biochemistry and shows great potential in synthesizing different kinds of peptides.^{2,12,15} Researchers have developed some strategies to synthesize peptides by manipulating the condensation of amino acids adsorbed on surfaces of inorganic materials. Generally, single-cycle heating yields primarily the cyclic anhydrides (or diketopiperazines, DKPs) and this has been considered a way to selectively synthesize substituted DKPs.^{10,12} Some amino

acids can also form oligomers when multiple wetting and drying cycles are used, and this has been proposed as a pathway for forming peptides at the very early stages of life.^{16–18} However, according to the literature, very few inorganic materials have ever been discovered and demonstrated to possess a unique surface that would facilitate the peptide synthesis with a high selectivity and a high yield.

Among all the inorganic oxide materials, silica is one of the most abundant minerals on earth and it has been extensively studied for decades due to its diverse properties, such as multiple structural forms and biocompatibility.^{19,20} It has a number of applications ranging from nanostructured materials to catalysts to acting as a medium for drug delivery.^{20,21} Amorphous silica nanomaterials, including fumed silica, mesoporous silica, and colloidal silica nanoparticles, are one class of synthetic silica materials, featuring small particle sizes and high surface areas.^{22–24} They have been studied extensively from experimental synthesis to structural characterization to biomedical applications.^{20,21,25–27} The adsorption and thermal

Received: April 6, 2017

Accepted: April 28, 2017

Published: April 28, 2017

condensation of amino acids on silica nanomaterials have attracted considerable attention during recent years to understand the interaction between biomolecules and nanoparticles, including the varying toxicity of different silica nanoparticle types.^{8,10,11,28–35}

While there are considerable experimental studies on ligand-capped mesoporous and colloidal silica nanoparticles,^{28,31,33,34,36} relatively less effort has been put into understanding the behaviors of amino acids as capping ligands on fumed silica nanoparticles.^{10,11,29,32,37} Fumed silica (Cab-O-Sil) nanoparticles are one class of synthetic nanomaterials composed of an amorphous structure with extensively high surface area and nanoscale size.²² They are prepared at high temperature by hydrolyzing silicon tetrachloride vapor in a flame followed by rapid quenching to room temperature. Many studies have been carried out on the surface chemistry at fumed silica nanoparticle interfaces because of the considerable utility of high surface area amorphous silicates.^{25,38–45} These studies have shown that the surface chemistry of fumed silica nanoparticles is very different from mesoporous and colloidal silica nanoparticles due to the presence of metastable strained ring structures in fumed silica that result from the fast quenching during the synthesis of the material in a flame. This unique property has been found to closely relate with the high surface reactivity of the fumed silica nanoparticles.^{46,47}

In our previous work, we have carried out a thorough investigation of alanine adsorption on fumed silica nanoparticles using a combination of thermal analysis and solid-state NMR spectroscopy.³² It was found that both the protonated amine group and the carboxyl group of alanine interact with the silanol group directly via hydrogen bonding when the sample is kept dry. Here, we focus on investigating the peptide bond formation reaction during the thermal condensation of alanine on fumed silica nanoparticles. Combining multiple spectroscopic techniques, including infrared (IR) and nuclear magnetic resonance (NMR) spectroscopy, it was discovered that alanine adsorbed on fumed silica nanoparticle surfaces is able to form a cyclic peptide, alanine anhydride, at ~ 170 °C with a high selectivity and a high yield of approximately 100%. This has not been achieved in previous efforts. This significant finding indicates the great potential of fumed silica nanoparticles in synthesizing peptides on solid surfaces with high yield. A recent report has demonstrated that a programmable condition can be used to synthesize oligopeptides with a yield $\sim 50\%$.¹⁸ Compared to that study, the method presented in this work shows an improved efficiency for peptide bond formation with a near 100% efficiency. To further unravel the mechanism of such high-selectivity and high-yield peptide formation on fumed silica nanoparticles, we carried out a comparative study of fumed and colloidal silica nanoparticles, and the results indicate that the high efficiency is very likely related to the intrinsic strained ring structures present at the interfaces of fumed silica nanoparticles that are not abundant in colloidal forms. This provides clear experimental evidence toward understanding the mechanism of “surface-catalyzed” peptide bond formation reactions on silica surfaces, since relatively less effort has been put forth on this topic compared to the extensive investigations on adsorption of amino acids on silicas.

EXPERIMENTAL SECTION

Materials. Fumed silica nanoparticles (~ 7 nm) with a BET (Brunauer, Emmett, and Teller) surface area of 395 ± 25 m²/g, tetraethoxysilane (TEOS, 98% purity), ethanol (absolute, >99.8%),

and pure L-alanine (99% purity) were purchased from Sigma-Aldrich. U-^[13C/15N]-L-alanine was purchased from Cambridge Isotopes Inc., and the stable isotope enrichment levels are 97–99%. All materials were used as received. In the following paragraphs, silica or SiO₂ refers to silica nanoparticles unless otherwise specified. Ala/FSN and ^{13C/15N}-Ala/FSN will refer to natural abundance alanine and ^{13C/15N}-labeled alanine adsorbed on fumed silica nanoparticles, respectively.

Adsorption of Alanine on Fumed Silica Nanoparticles.

Fumed silica nanoparticles were first heated to 500 °C overnight to remove impurities on the surface. In a typical adsorption procedure, 75 mg of fumed silica nanoparticles were mixed with different amounts of L-alanine in 5.0 mL of DI water, and the mixture was stirred at room temperature for over 3 h to ensure that the adsorption reached equilibrium. Nanoparticles were then separated by centrifugation at 6000 rpm for 1 h and dried under vacuum at room temperature overnight. Samples were prepared from solutions of various concentrations and are noted as Ala/FSN-*x*M, respectively, where *x* refers to the alanine concentration in the adsorption solutions (in mol L⁻¹).

In this work, ^{13C/15N}-Ala/FSN-0.03M was prepared for solid-state NMR investigations. A 120.0 mg portion of fumed silica nanoparticles was mixed with 21.6 mg of ^{13C/15N}-L-alanine in 8.0 mL of DI water, and the pH value remained constant at 6.7. The suspension was then stirred for over 3 h to reach equilibrium. The mixture was then centrifuged at 6000 rpm for 1 h, and the remaining powders were allowed to vacuum-dry at room temperature overnight. The ^{13C/15N}-Ala/FSN samples were then packed first in a NMR rotor and further vacuum-dried with the cap removed (0.001 mbar) for 1 month in order to remove the physisorbed water. NMR investigations on dried samples were carried out immediately after completion of the drying process. No obvious rehydration was found in this work during the course of solid-state NMR experiments.

For preparation of Ala/FSN-0.03M for thermal condensation studies, 300 mg of fumed silica nanoparticles were mixed with 53.5 mg of L-alanine in 20.0 mL of DI water, and the mixture was stirred at room temperature for over 3 h.

Synthesis of Colloidal Silica Nanoparticles. Colloidal silica nanoparticles (CSN) with a size of ~ 38 nm were synthesized using the well-established method developed by Stöber et al.⁴⁸ Briefly, 0.17 M tetraethoxysilane was hydrolyzed and condensed in a 100.0 mL ethanol solution with 0.5 M NH₃ and 2.0 M H₂O for 12 h at room temperature. The formed silica nanoparticles were then dialyzed against ultrapure water and stored at a final concentration of 1.6 mg/mL.

Adsorption of Alanine on Colloidal Silica Nanoparticles. A 1.0 mg portion of pure L-alanine was added to a 100 mL solution of colloidal silica nanoparticles ([CSN] ~ 1.6 mg/mL) and the solution was stirred in excess of 3 h to reach equilibrium. Colloidal silica nanoparticles with alanine adsorbed on the surface (Ala/CSN) were obtained after drying from the solution at room temperature.

Thermal Condensation. Dried silica nanoparticles with alanine adsorbed on the surface were incubated (heated) in an oven at 170 °C for 3 h. After incubation, the peptides were washed with DI water followed by centrifugation at 14 000 rpm for 30 min. The supernatant fluid was collected and dried to obtain the solid powder. The resulting solid powder was dissolved in a 700 μ L of H₂O/D₂O (90/10) solution and transferred to a 5 mm NMR tube. Solid-state NMR spectroscopy was used to probe the thermal condensation of alanine on fumed silica nanoparticles. Briefly, ^{13C/15N}-Ala/FSN-0.03M was first packed in the rotor followed by incubation at 170 °C for 3 h with the rotor cap removed. The rotor was then cooled down to room temperature and sealed for solid-state NMR characterization.

Thermal Analysis. Thermal gravimetric analysis (TGA) experiments were performed with a TGA2950 (TA Instrument Inc.) instrument under dry N₂ flow (30 mL/min for furnace and 30 mL/min for balance). For each experiment, 5–10 mg of sample was used and a heating rate of 5 °C/min was utilized. Before each experiment, the sample was kept under a nitrogen flow for a minimum of 10 min to obtain a stable baseline.

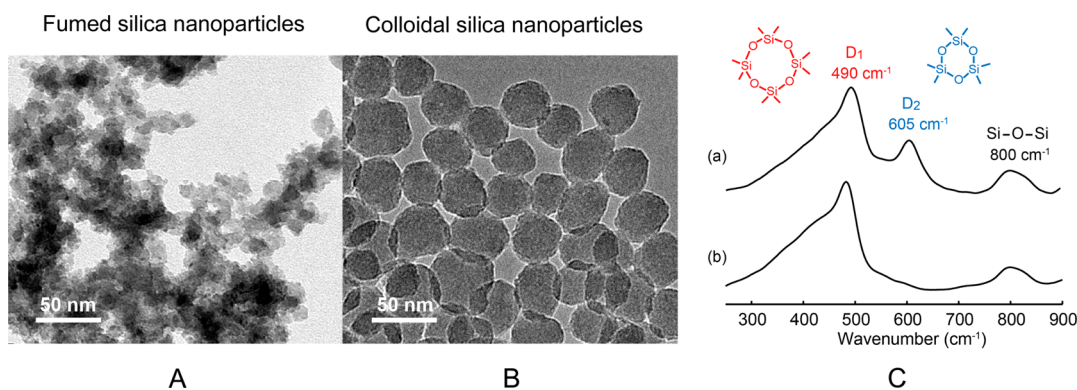


Figure 1. TEM images of (A) fumed silica nanoparticles and (B) colloidal silica nanoparticles. (C) Raman spectra of silica nanoparticles: (a) fumed silica and (b) colloidal silica nanoparticles.

Infrared (IR) Spectroscopy. IR spectra were recorded using a PerkinElmer FTIR spectrometer with a diamond ATR accessory. The instrument carries a MIR light source of 300–8000 cm^{-1} , an OptKBr beam splitter (400–7800 cm^{-1}), and a LiTaO₃ detector (370–15 700 cm^{-1}). The spectra were collected with a spectral window of 400–4000 cm^{-1} , a resolution of 4 cm^{-1} , and 32 scans.

Raman Spectroscopy. Raman spectroscopy was performed on a home-built system utilizing a 532 nm laser and triple-grating monochromator (SpectraPro 300i, Action Research). The laser beam was focused onto the sample through a Mitutoyo M Plan Apo 50 \times objective with 0.42 NA. All spectra were collected with a laser power of 50 mW, an exposure time of 30 s, and 10 scans.

Transmission Electron Microscopy (TEM). The size and morphology of the silica nanoparticles were characterized using a Philips CM200-FEG high-resolution transmission electron microscope (TEM) operating at a bias voltage of 200 kV. The TEM samples were prepared by dipping carbon-coated copper grids in silica nanoparticle dispersion and drying them in air for a minimum of 2 h.

Solid-State Nuclear Magnetic Resonance (NMR) Spectroscopy. Solid-state NMR spectroscopy experiments were performed on a Varian VNMRs 400 MHz spectrometer with a 1.6 mm triple-resonance probe operating in triple-resonance (¹H/¹³C/¹⁵N) mode at a MAS speed of 35 kHz. ¹H → ¹³C and ¹H → ¹⁵N cross-polarization magic-angle-spinning (CP-MAS) experiments and two-dimensional (2D) ¹H–¹³C heteronuclear correlation (HETCOR) and ¹H–¹⁵N HETCOR NMR experiments were applied to characterize all samples. The CP condition for ¹H → ¹³C CP-MAS NMR experiments consisted of a 1.6 μs ¹H $\pi/2$ pulse, followed by a 1.0 ms/2.0 ms ramped (13%) ¹H spin-lock pulse with 75 kHz rf field strength. The experiments were performed with a 25 kHz sweep width, a recycle delay of 3.0 s, and a two-pulse phase-modulated⁴⁹ (TPPM) ¹H decoupling level with 156 kHz rf field strength. The CP condition for ¹H → ¹⁵N CP-MAS NMR experiments consisted of a 1.6 μs ¹H $\pi/2$ pulse, followed by a 1.0 ms/2.0 ms ramped (10%) ¹H spin-lock pulse with 95 kHz rf field strength. The experiments were performed with a 25 kHz sweep width, a recycle delay of 3.0 s, and the same ¹H decoupling conditions described above. A contact time of 1.0 ms was applied in ¹H → ¹³C and ¹H → ¹⁵N CP-MAS NMR experiments for pure alanine, while a contact of 2.0 ms was applied for ¹³C/¹⁵N-Ala/FSN-0.03M. 2D ¹H–¹³C HETCOR and 2D ¹H–¹⁵N HETCOR NMR experiments were carried out on ¹³C/¹⁵N-Ala/FSN samples. The experimental CP condition and TPPM ¹H decoupling parameters for 2D HETCOR NMR experiments were identical to 1D CP-MAS NMR experiments with the exception of contact times. The 2D ¹H–¹³C HETCOR NMR experiment was performed with a contact time of 2.0 ms, a recycle delay of 3.0 s, sweep widths of 25 kHz and 10 kHz for direct and indirect dimensions, respectively, and 32 complex t_1 points. 2D ¹H–¹⁵N HETCOR NMR experiment was performed with a contact time of 2.0 ms, a recycle delay of 3.0 s, a sweep width of 10 kHz for both dimensions, and 32 complex t_1 points.

In all experiments, the chemical shifts of ¹H, ¹³C, and ¹⁵N were indirectly referenced to adamantane (¹H, 1.63 ppm; ¹³C, 38.6 ppm)

and glycine (¹⁵N, 32.6 ppm), respectively.^{50,51} The line-broadening (lb) was set to 25 Hz for ¹H → ¹³C CP-MAS spectra, ¹H → ¹⁵N CP-MAS spectra, and 2D ¹H–¹³C HETCOR spectra and to 50 Hz for 2D ¹H–¹⁵N HETCOR spectra.

Solution NMR Spectroscopy. Solution NMR spectroscopy experiments were performed on a VNMRs 500 MHz spectrometer with a 5 mm triple-resonance probe operating in triple-resonance (¹H/¹³C/¹⁵N) mode. ¹H NMR spectra were collected with a sweep width of 8012.8 Hz, an acquisition time of 2.045s, a recycle delay of 5.0 s, and 512 scans. ¹H–¹³C HSQC spectra were collected with a recycle delay of 1.0 s, sweep widths of 8012.8 and 25141.4 Hz for direct and indirect dimensions, respectively, and 256 complex t_1 points.

RESULTS AND DISCUSSION

Morphology and Structure of Amorphous Silica Nanoparticles. Amorphous silica nanoparticles are typically prepared by two main methods: high-temperature flame pyrolysis to form so-called fumed silica nanoparticles and condensation of tetraethyl orthosilicate in aqueous solution or under hydrothermal conditions to form colloidal (Stöber) or mesoporous silica nanoparticles. Both fumed and colloidal silica nanoparticles were investigated to compare their efficiency of surface catalysis in forming peptide bonds for alanine. Fumed silica nanoparticles are obtained by hydrolyzing silicon tetrachloride vapor in a flame followed by rapid quenching to room temperature. This process generates small primary particles with diameters from a few to tens of nanometers and are best described as ramified, chainlike aggregates (Figure 1A). The fumed silica nanoparticles used in this study possess an average particle size \sim 7 nm according to the manufacturer. Colloidal silica nanoparticles are synthesized according to the Stöber method and are nonaggregated, monodisperse spherical nanoparticles (Figure 1B). The average size of the Stöber silica nanoparticles is determined to be \sim 38 nm in diameter. Because of the much smaller size of primary particles, fumed silica nanoparticles feature a high surface area up to \sim 390 m²/g compared to the synthesized colloidal silica nanoparticle whose surface area is only \sim 60 m²/g.

Raman spectroscopy was applied to investigate the surface structures of the two types of silica nanoparticles, and the spectra are shown in Figure 1C. Comparison between fumed silica and Stöber silica nanoparticles indicates that their surface properties are different. For fumed silica nanoparticles, two significant bands at \sim 490 cm^{-1} (D₁) and 605 cm^{-1} (D₂) are observed that can be attributed to four- and three-membered siloxane rings, respectively.⁴⁵ There is also a broad band centered at \sim 450 cm^{-1} attributed to the five-member and larger

siloxane rings. Stöber silica nanoparticles have a prominent band at $\sim 490\text{ cm}^{-1}$ but no well-resolved band at $\sim 605\text{ cm}^{-1}$, indicating the absence of three-membered rings at the surface. This result is in good agreement with a previous experimental finding.⁴⁶ The relatively large population of strained three-membered rings on fumed silica nanoparticle surfaces is due to the rapid quenching of silica materials at very high temperatures during the synthesis in a flame. This process freezes the silica structure in some strained structures, such as three-membered rings, and this is also observed for Aerosil fumed silica with particle diameters of 14 and 40 nm.⁴⁵ Stöber silica nanoparticles are synthesized in solution via continuous condensation reactions, and they are principally composed of unstrained four-membered and larger rings that are more stable and less reactive. The absence of three-membered ring is also characteristic of other solution-derived silica nanoparticles, including mesoporous silica and silica gels.⁵²

Thermal Condensation of Alanine on Fumed Silica Nanoparticles. Amino acids can undergo thermal condensation in bulk and on surfaces of inorganic materials such as silica, aluminum, and minerals.^{11,12,14} Differential thermal gravimetric (DTG) analysis is used as a primary technique here to characterize the thermal behavior of variable samples. It shows a rate of mass loss versus temperature during the heating of samples. According to the previous studies,³² for bulk alanine, no obvious thermal event was detected below 200 °C, and one broad peak composed of multiple components appeared around 270 °C. The thermal condensation process ($\sim 210\text{ °C}$) is overlapped by other thermal events like decomposition and is not easily recognized. However, for alanine adsorbed on fumed silica nanoparticles, a well-distinguished peak is observed around 170 °C at a heating rate of 5 °C/min, which is due to the thermal condensation of alanine forming peptide bonds. The other peaks observed above 220 °C correspond to a complicated thermal degradation process with the elimination of NH_3 and CO_2 similar to bulk alanine and will not be further discussed in this paper. Table 1 summarizes the thermal

Table 1. Summary of Alanine Adsorption and Thermal Condensation on Fumed Silica Nanoparticles from Thermal Analysis²⁹

alanine concn (M)	DTG peak values (°C)		adsorbed alanine (%)
	peak I	peak II	
0.01			2.8
0.03	171	280	4.2
0.05	171	279	5.0
0.08	172	269	7.0
0.10	173	263	8.7
0.15	171	253	10.5

condensation results as a function of initial alanine concentration in the prepared solutions. With the increasing amount of alanine on the surface, the temperature of thermal condensation had little change, indicating that the adsorbed alanine is the main species contributing to the thermal condensation. Here, we focus primarily on Ala/FSN-0.03M, since it was shown to be a monolayer adsorbed sample [Figure S1, Supporting Information (SI)].³² By lowering the heating rate from 5 to 1 °C/min, the thermal condensation peak was detected at an even lower temperature around 149 °C (Figure 2A). This finding indicates that the fumed silica nanoparticle surfaces are able to catalyze the formation of peptide bond and

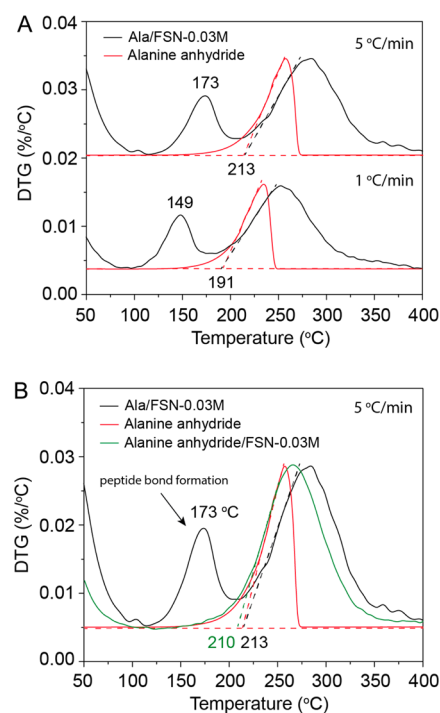


Figure 2. (A) DTG curves for Ala/FSN-0.03M (black) and alanine anhydride (red) with two different heating rates (5 and 1 °C/min). (B) DTG curves for Ala/FSN-0.03M (black), alanine anhydride (red), and alanine anhydride/FSN-0.03M (green) with a heating rate of 5 °C/min.

lower dramatically the thermal condensation temperature of alanine. The product of thermal condensation is very likely alanine anhydride, since it has been proposed previously that a single-cycle heating yields primarily the cyclic anhydrides (or DKPs). The thermal analysis results of alanine anhydride and alanine anhydride adsorbed on fumed silica nanoparticles (alanine anhydride/FSN-0.03M) support this assumption, since the onset temperature of alanine anhydride ($\sim 213\text{ °C}$) degradation agrees well with the onset temperature of thermal degradation ($\sim 213\text{ °C}$) for alanine adsorbed on fumed silica nanoparticles (Figure 2). However, it is in fact difficult to provide convincing evidence identifying the product of thermal condensation on the basis of thermal analysis only. Hence, additional techniques such as NMR spectroscopy and IR spectroscopy were used in this study to further characterize the product produced.

NMR and IR spectroscopies were applied as advanced techniques for investigating the thermal condensation of alanine on the fumed silica nanoparticle surfaces. $^1\text{H} \rightarrow ^{13}\text{C}$ and $^1\text{H} \rightarrow ^{15}\text{N}$ CP-MAS solid-state NMR experiments were performed on isotope-labeled samples ($^{13}\text{C}/^{15}\text{N}$ -Ala/FSN-0.03M) following thermal condensation, and the results are shown in Figure 3. After thermal incubation at 170 °C for 3 h, the intensities of the ^{13}C resonance at 176.0 ppm and ^{15}N resonance at 43.3 ppm decreased and two new resonances appear due to peptide bond formation during thermal condensation. The ^{13}C resonance at 171.1 ppm and ^{15}N resonance at 120.2 ppm were assigned to the carbonyl group and the amide group of the formed peptide, respectively (Figure 3d). The ^{13}C resonance of the carbonyl group is consistent with the ^{13}C resonance of the carbonyl group of alanine anhydride (Figure 3b), indicating the formation of alanine anhydride. Furthermore, the intensity of the carboxyl

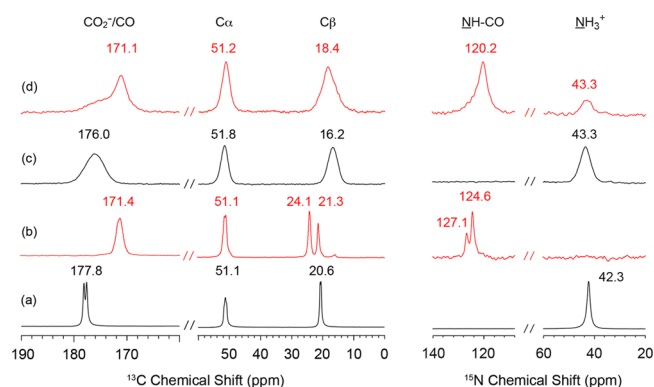


Figure 3. $^1\text{H} \rightarrow ^{13}\text{C}$ and $^1\text{H} \rightarrow ^{15}\text{N}$ CP-MAS spectra of (a) $^{13}\text{C}/^{15}\text{N}$ -alanine, (b) alanine anhydride, (c) $^{13}\text{C}/^{15}\text{N}$ -Ala/FSN-0.03M, and (d) $^{13}\text{C}/^{15}\text{N}$ -Ala/FSN-0.03M incubated at $170\text{ }^\circ\text{C}$ for 3 h. The spectra of $^{13}\text{C}/^{15}\text{N}$ -alanine and $^{13}\text{C}/^{15}\text{N}$ -Ala/FSN-0.03M are shown in black, while the spectra of alanine anhydride and $^{13}\text{C}/^{15}\text{N}$ -Ala/FSN-0.03M incubated at $170\text{ }^\circ\text{C}$ for 3 h are shown in red.

group decreased after thermal condensation, showing a small broad peak overlaid with the strong carbonyl peak assigned to the peptide. This indicates that the vast majority of adsorbed alanine was converted to peptides. This point was further confirmed by ^{15}N solid-state NMR spectroscopy, where a weak ^{15}N signal for NH_3^+ groups and a strong signal for peptide amide bonds were observed following thermal condensation. The ^{15}N resonance of the amide group in the formed peptide shows ~ 3 ppm difference compared to the ^{15}N resonance of the amide group for crystalline alanine dipeptide (~ 123 ppm).⁵³ However, it has a similar ^{15}N resonance to the amide group of alanine residue in silk protein (~ 120 ppm) that is involved in strong hydrogen bonding.⁵⁴ This indicates that the formed peptide may interact with the silica surfaces via amide groups forming hydrogen bonds to the silica surface. According to 2D $^1\text{H}-^{13}\text{C}$ and 2D $^1\text{H}-^{15}\text{N}$ HETCOR NMR spectra (Figure S2, SI), the ^1H resonance of the amide group was detected at 6.4 ppm while the ^1H resonances of α -CH and β - CH_3 are at 3.2 and 1.2 ppm, respectively. This smaller ^1H resonance of amide proton provides further evidence that amide protons are involved in a hydrogen bond network with the silica surfaces.³⁶ In CP-MAS spectra, a considerable CP signal was observed for unreacted alanine. However, the CP-MAS spectroscopy is not quantitative, and a stronger than expected signal could be observed for the unreacted alanine because it exhibits a higher degree of rigidity compared to the formed peptide. Furthermore, for in situ solid-state NMR characterization, the sample was packed tightly in the rotor, where water could not evaporate freely during the thermal incubation. As a result, the thermal condensation reaction might be slower in the NMR rotor and it needs more time to complete compared to that in an open space.

Similar to the results from solid-state NMR, IR spectroscopy also shows alanine anhydride formed during thermal condensation (Figure 4, Table 2). The band for $\text{O}=\text{C}-\text{O}$ stretching (1624 cm^{-1}) disappeared and two well-defined bands appear at 1668 and 1689 cm^{-1} , which are assigned to the $\text{C}=\text{O}$ stretching of amide I.^{55,56} This result indicates that alanine did undergo thermal condensation at the interfaces and form a peptide bond. Further, after comparing the spectra of Ala/FSN-0.03M following thermal incubation with the pure alanine anhydride, it is compelling to find that vibrational bands

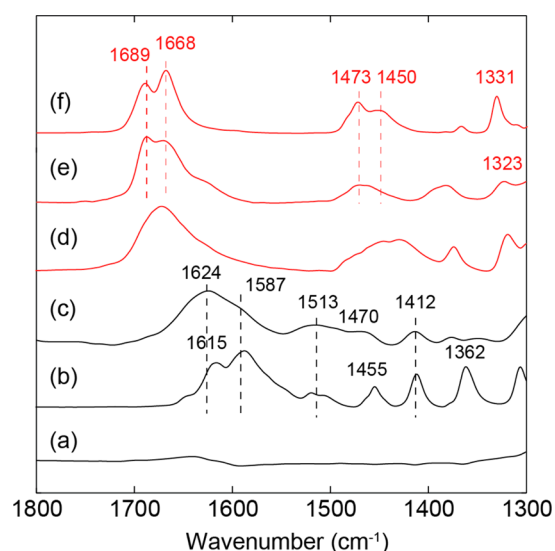


Figure 4. FTIR spectra of (a) fumed silica nanoparticles, (b) alanine, (c) Ala/FSN-0.03M, (d) Ala/FSN-0.03M incubated at $170\text{ }^\circ\text{C}$ for 3 h, (e) product washed off nanoparticles after thermal incubation, and (f) alanine anhydride. The spectra of Ala/FSN-0.03M incubated at $170\text{ }^\circ\text{C}$ for 3 h, product washed off nanoparticles after thermal incubation, and alanine anhydride are shown in red.

Table 2. Assignments of FTIR Bands^{55,56}

band position (cm^{-1})	assignments
1689	amide I $\text{C}=\text{O}$ stretching
1668	amide I $\text{C}=\text{O}$ stretching
1624, 1615	$\text{O}=\text{C}-\text{O}$ stretching
1587	NH_3^+ stretching
1513	NH_3^+ stretching
1473	ring stretching
1455	CH_3 stretching
1412	CH_3 stretching
1362	$\text{O}=\text{C}-\text{O}$ stretching

identified from two spectra are very similar, indicating that the formed peptide is alanine anhydride, in agreement with the solid-state NMR interpretation.

The product formed during the thermal condensation was then washed off the fumed silica nanoparticle surfaces and characterized by solution NMR spectroscopy. According to the ^1H NMR spectra shown in Figure 5, the ^1H resonances and splitting patterns of the formed peptide are identical to those of pure alanine anhydride (Figure 5a). This result provides strong evidence that the peptide formed during the thermal condensation is alanine anhydride and that almost all of the adsorbed alanine was converted to alanine anhydride, one of the simplest cyclic peptides. This finding was further confirmed by $^1\text{H}-^{13}\text{C}$ HSQC NMR spectra that indicated that the formed peptide is alanine anhydride (see Figure S3, SI). In summary, this combination of experiments has shown that fumed silica nanoparticle surfaces are able to serve as catalysts for converting alanine to alanine anhydride via thermal condensation, significantly lowering the reaction temperature (Figure 6). Moreover, the alanine anhydride yield is estimated to be 98.8% from the ^1H NMR spectrum (Figure S4, SI), indicating the high efficiency and selectivity of fumed silica nanoparticles in catalyzing peptide bond formation. It is also worth noting here that a very small amount of unreacted alanine and minor

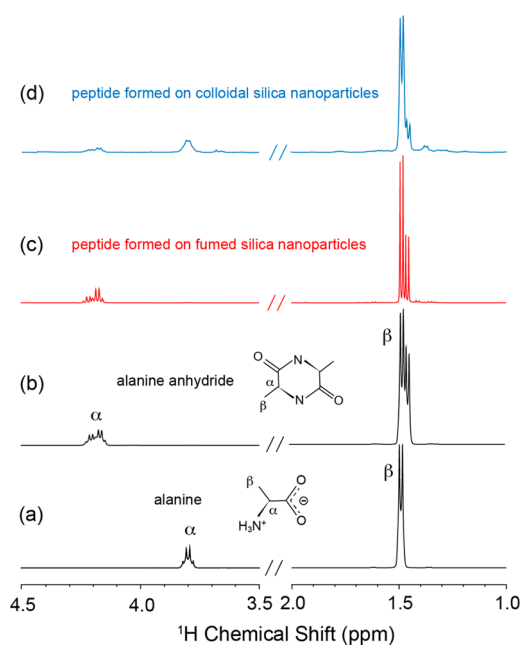


Figure 5. ¹H NMR spectra of (a) alanine, (b) alanine anhydride, (c) peptide formed on fumed silica nanoparticles (red), and (d) peptide formed on colloidal silica nanoparticles (blue).

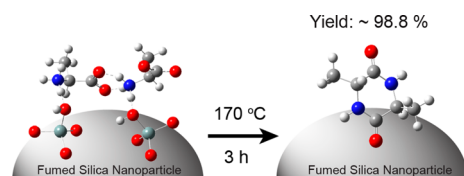


Figure 6. Schematic representation of thermal condensation of alanine at 170 °C forming alanine anhydride on fumed silica nanoparticles.

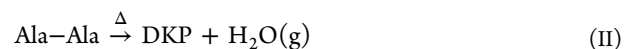
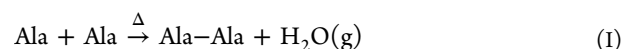
degradation indicated by the multiplicity of ¹H resonances were observed in the ¹H NMR spectrum (see Figure S4, SI).

Comparison Between Fumed Silica Nanoparticles and Colloidal Silica Nanoparticles on Surface-Catalyzed Peptide Bond Formation Reaction. From the present study on thermal condensation of alanine on fumed silica nanoparticles, it is illustrated that fumed silica nanoparticles have exceptionally high efficiency for surface-catalyzed peptide bond formation reaction. Here, a simple question then arises: Do other types of amorphous silica nanomaterials have the same property? To answer this question, we decided to investigate another type of the most common silica nanomaterials, colloidal silica nanoparticles. The colloidal silica nanoparticles were synthesized following the classical Stöber method, and they possess a well-defined spherical shape with an average diameter around 38 nm. The surface area is much lower than that of fumed silica nanoparticles, resulting in a much lower amount of adsorbed alanine on the surfaces. The TGA profile indicates that the adsorbed alanine is less than 2 wt %, and the DTG curve does not exhibit a clear peak around 170 °C attributed to the peptide bond formation reaction (see Figure S5, SI). Figure Sd shows the ¹H NMR spectrum of the product from the thermal condensation on Stöber silica nanoparticles. The multiple small ¹H resonances at 4.2 ppm indicate the formation of alanine anhydride, but the yield is low (~51.2%). The vast majority of adsorbed alanine still remained unreacted on the surface, as indicated by the well-defined ¹H

resonance at 3.8 ppm. This result is further supported by IR spectroscopy showing that the alanine is the main species present on the colloidal silica nanoparticle surfaces after thermal condensation (Figure S6, SI). On the basis of the comparison between the surface-catalyzed peptide bond formation reaction on the fumed silica nanoparticles and colloidal silica nanoparticles, it is concluded that fumed silica nanoparticles possess a better efficiency than colloidal silica nanoparticles in forming the peptide bond, and it has an efficiency of 98.8% and a high selectivity in the case of synthesizing alanine anhydride from alanine.

Catalytic Property of Fumed Silica Nanoparticle Surfaces in Peptide Bond Formation. It has been demonstrated that some amino acids are able to undergo thermal condensation in the presence of inorganic oxides or mineral surfaces, such as silica, alumina, or clay, since the phenomenon was first discovered in 1978.^{1–3} In this work, we showed a good example in which alanine can undergo thermal condensation on fumed silica nanoparticles, forming peptide bonds. More significantly, the formed peptide is almost pure alanine anhydride, the product of alanine dimerization. Though this type of surface-catalyzed peptide bond formation reaction has been shown many times during the past decades, the mechanism of the catalysis still remains unclear. However, two things appear to be certain for the surface-catalyzed peptide bond formation reaction: first, the peptide bond formation reaction from amino acids is thermodynamically unfavored in aqueous solutions;⁵⁷ however, it can be achieved in the adsorbed state on surfaces where the water activity is low.¹⁴ Second, keeping water activity low is the driving force for the condensation reaction, because it releases water as a product. In this part of the discussion, we focus on understanding the role of the silica nanoparticle surfaces in catalyzing the peptide bond formation by combining the findings from previous research and the results we obtained in this work. Additionally, we also discuss the possible reasons for the high efficiency of fumed silica nanoparticles. In the discussion, DKP will be used to stand for alanine anhydride, since it is frequently used to indicate the cyclized form of alanine.

Since the formation of alanine DKP involves the formation of two peptide bonds, a possible two-step reaction mechanism has been proposed:



In **step I**, adsorbed alanine forms linear alanine dipeptide and it reacts further by cyclization to DKP in **step II**. Previous studies on glycine adsorbed on silica have shown that the cyclization happens at a lower temperature than its initial linear dimerization.⁹ So it might be the same case for alanine here in this work, where the linear alanine dipeptide is formed and it would immediately undergo further cyclization to DKP at elevated temperature.

According to the DTG results, the adsorbed alanine is the primary reservoir for DKP formation at ~170 °C with a heating rate of 5 °C/min, since the crystalline alanine shows no significant thermal event below 200 °C. Furthermore, the little change in temperatures of thermal condensation with the increasing amount of alanine on surfaces also indicates that the adsorbed alanine is the main contributor for the condensation reaction. On the basis of this finding, understanding the

mechanism of DKP formation lies with unraveling the interaction between adsorbed alanine and surface groups and the behavior of adsorbed alanine at the interfaces during thermal incubation. For the interaction between adsorbed alanine and surface groups, solid-state NMR spectroscopy has provided some clues regarding the binding state of alanine, and more details can be found in our previous work.³² At very low water activity levels, the reorientation of adsorbed alanine is restricted to some degree and it interacts with surface silanol groups via the carboxyl group and protonated amine group (NH_3^+). This is likely the model describing the surface chemistry at the very early stage of thermal incubation, when the sample is being heated up to 100 °C, since most physisorbed water is removed from the surfaces of nanoparticles. In the following thermal incubation with the temperature increasing up to 170 °C, the mobility of the adsorbed alanine increases, since the alanine–surface interaction may be broken and re-formed during this stage. This thermally driven reorientation makes alanine molecules interact frequently with each other at the interfaces. Surface silanol groups are also able to serve as the active sites for interacting with both carboxylate groups and amine groups, which may lower the energy barrier for the subsequent peptide bond formation reaction between alanine molecules. When the temperature reaches the point of overcoming the energy barrier of the peptide bond formation reaction (~ 170 °C with a heating rate of 5 °C in this work), the condensation is triggered and the peptide bond forms. This proposed mechanism may give an explanation for forming the peptide bond at a lower temperature on silica nanoparticle surfaces, including fumed silica nanoparticles and colloidal silica nanoparticles, compared to that in the bulk.

To further understand the reason for the ultrahigh efficiency for fumed silica nanoparticles, Raman spectra of alanine adsorbed on fumed silica nanoparticles after incubation at 170 °C for 3 h were collected and compared to spectra of the fumed silica nanoparticles (Figure 7B). Adsorbed alanine is not

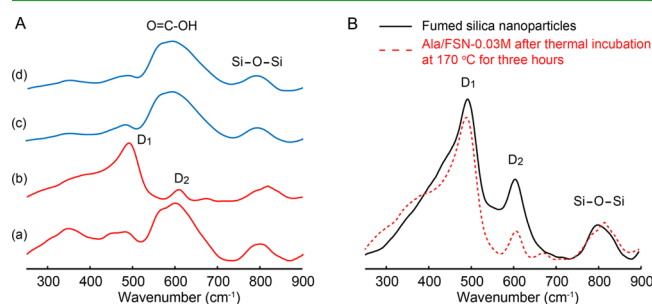


Figure 7. (A) Raman spectra of (a) Ala/FSN-0.03M, (b) Ala/FSN-0.03M after thermal incubation at 170 °C for 3 h, (c) Ala/CSN, and (d) Ala/CSN after thermal incubation at 170 °C for 3 h. The spectra for FSN and CSN are shown in red and blue, respectively. (B) Raman spectra of fumed silica (solid line) and Ala/FSN-0.03M after thermal incubation at 170 °C for 3 h (dashed line). The spectra were normalized using the peak area of the Si–O–Si band at ~ 800 cm^{-1} .

present in crystalline form, since no characteristic resonances were found for alanine in crystalline form (Figure S7, SI). After thermal incubation, alanine converts to alanine anhydride at the interface of fumed silica nanoparticles (Figure 7A), where the amine group and carboxylate group form the amide bond. The formed alanine anhydride is believed to exhibit weaker interactions with surface silanol groups compared to alanine.³²

As a result, the formed alanine anhydride was barely detected in the spectra. However, the D_1 and D_2 bands of silica surface groups are clearly observed. The spectra were normalized to the amplitude of the band centered at ~ 800 cm^{-1} to carry out a quantitative analysis. This protocol is suitable and reliable because the band at ~ 800 cm^{-1} , assigned to the symmetric stretching vibration of the Si–O–Si group, is very stable and this protocol has been proven in previous studies.^{45,58,59} The intensity of the D_2 band showed a significant decrease, while the intensity of the D_1 band did not vary to any appreciable extent. Since the D_2 band is assigned primarily to the three-membered siloxane ring structure, this result indicates that the content of three-membered siloxane rings decreased during the processing and thermal condensation. It has been suggested recently, due to electron paramagnetic resonance (EPR), that the surface three-membered siloxane rings of fumed silica can form radicals via homolytic cleavage of siloxane bonds that can further generate hydroxyl radicals when hydrolyzed.⁴⁶ On the basis of this finding, it may be reasonable to propose that surface radicals may be generated on fumed silica nanoparticle surfaces during processing and then catalyze the peptide bond formation reaction significantly. The contribution of radicals to the high efficiency of fumed silica nanoparticles still remains uncertain and it needs more investigation; however, it is important to note here that fumed silica nanoparticles, in contrast to colloidal silica nanoparticles, have a considerable amount of surface three-membered siloxane rings, which can potentially serve as a reservoir for surface radicals. In addition, a recent simulation study has proposed another mechanism in which strained siloxane rings react first with carboxylic acids, forming a $-\text{Si}-\text{O}-\text{C}(=\text{O})-$ surface mixed anhydride, and the surface mixed anhydride undergoes further reaction with amines to form peptide bonds.⁶⁰ For more details on the mechanism, we will continue our investigation and address more details in our future reports.

CONCLUSION

In this work, we carried out a thorough investigation on the thermal condensation of alanine on fumed silica nanoparticles. It is found that the adsorbed alanine can undergo a surface-catalyzed thermal condensation at around 170 °C, forming alanine anhydride with a very high yield of 98.8%. This finding suggests a potential way of synthesizing peptides with high efficiency and high selectivity in inorganic nanostructured interfaces. To further understand the fundamental origin of such high-selectivity and high-yield peptide formation on fumed silica nanoparticles, a comparative study was carried out between fumed silica nanoparticles and colloidal silica nanoparticles. It is found that the high efficiency for fumed silica nanoparticles is likely related to the intrinsic strained ring structures present on the nanoparticles surfaces. In addition, in this work, NMR, IR, and Raman spectroscopies have been successfully applied to characterize the alanine–silica interfaces, which demonstrates that these techniques can be used in the future for more bioinorganic interface research.

ASSOCIATED CONTENT

Supporting Information

The Supporting Information is available free of charge on the ACS Publications website at DOI: 10.1021/acsami.7b04887.

The amount of alanine adsorbed on silica as a function of the initial concentration of alanine at room temperature

and pH 6.7; $^1\text{H} \rightarrow ^{13}\text{C}$ and $^1\text{H} \rightarrow ^{15}\text{N}$ 2D-HETCOR NMR spectra of $^{13}\text{C}/^{15}\text{N}$ -Ala/FSN-0.03M and $^{13}\text{C}/^{15}\text{N}$ -Ala/FSN-0.03M incubated at 170 °C for 3 h; ^1H - ^{13}C HSQC NMR spectra of alanine anhydride and peptide formed at the surface of fumed silica nanoparticles by incubating with Ala/FSN-0.03M at 170 °C for 3 h; ^1H NMR spectra of alanine and peptide formed at the surface of fumed silica nanoparticles by incubating with Ala/FSN-0.03M at 170 °C for 3 h; TGA and DTG curves of alanine adsorbed on colloidal silica nanoparticles; FTIR spectra of colloidal silica nanoparticles, alanine, alanine adsorbed on colloidal silica nanoparticles, alanine adsorbed on colloidal silica nanoparticles incubated at 170 °C for 3 h, and alanine anhydride; Raman spectra of alanine and alanine anhydride in crystalline form (PDF)

AUTHOR INFORMATION

Corresponding Authors

*C.G. e-mail: Chengchen.Guo@asu.edu.

*G.P.H. e-mail: gholland@mail.sdsu.edu.

ORCID

Chengchen Guo: 0000-0001-9253-3469

Jeffery L. Yarger: 0000-0002-7385-5400

Notes

The authors declare no competing financial interest.

ACKNOWLEDGMENTS

The research was supported by grants from the National Science Foundation (CHE-1011937, DMR-1264801). We thank Dr. Brian Cherry for help with NMR instrumentation, student training, and scientific discussion.

REFERENCES

- (1) Zaia, D. A. M. A Review of Adsorption of Amino Acids on Minerals: Was It Important for Origin of Life? *Amino Acids* **2004**, *27* (1), 113–118.
- (2) Lambert, J.-F. Adsorption and Polymerization of Amino Acids on Mineral Surfaces: a Review. *Origins Life Evol. Biospheres* **2008**, *38* (3), 211–242.
- (3) Lahav, N.; White, D.; Chang, S. Peptide Formation in the Prebiotic Era: Thermal Condensation of Glycine in Fluctuating Clay Environments. *Science* **1978**, *201* (4350), 67–69.
- (4) Hudson, S.; Cooney, J.; Magner, E. Proteins in Mesoporous Silicates. *Angew. Chem., Int. Ed.* **2008**, *47* (45), 8582–8594.
- (5) Lee, C.-H.; Lin, T.-S.; Mou, C. Mesoporous Materials for Encapsulating Enzymes. *Nano Today* **2009**, *4* (2), 165–179.
- (6) Ashley, C. E.; Carnes, E. C.; Phillips, G. K.; Padilla, D.; Durfee, P. N.; Brown, P. A.; Hanna, T. N.; Liu, J.; Phillips, B.; Carter, M. B.; Carroll, N. J.; Jiang, X.; Dunphy, D. R.; Willman, C. L.; Petsev, D. N.; Evans, D. G.; Parikh, A. N.; Chackerian, B.; Wharton, W.; Peabody, D. S.; Brinker, C. J. The Targeted Delivery of Multicomponent Cargos to Cancer Cells by Nanoporous Particle-Supported Lipid Bilayers. *Nat. Mater.* **2011**, *10* (5), 389–397.
- (7) Ashley, C. E.; Carnes, E. C.; Epler, K. E.; Padilla, D. P.; Phillips, G. K.; Castillo, R. E.; Wilkinson, D. C.; Wilkinson, B. S.; Burgard, C. A.; Kalinich, R. M.; Townson, J. L.; Chackerian, B.; Willman, C. L.; Peabody, D. S.; Wharton, W.; Brinker, C. J. Delivery of Small Interfering RNA by Peptide-Targeted Mesoporous Silica Nanoparticle-Supported Lipid Bilayers. *ACS Nano* **2012**, *6* (3), 2174–2188.
- (8) Rimola, A.; Costa, D.; Sodupe, M.; Lambert, J.-F.; Ugliengo, P. Silica Surface Features and Their Role in the Adsorption of Biomolecules: Computational Modeling and Experiments. *Chem. Rev.* **2013**, *113* (6), 4216–4313.

(9) Orgel, L. E. Polymerization on the Rocks: Theoretical Introduction. *Origins Life Evol. Biospheres* **1998**, *28*, 227–234.

(10) Meng, M.; Stievano, L.; Lambert, J.-F. Adsorption and Thermal Condensation Mechanisms of Amino Acids on Oxide Supports. 1. Glycine on Silica. *Langmuir* **2004**, *20* (3), 914–923.

(11) Bouchoucha, M.; Jaber, M.; Onfroy, T.; Lambert, J.-F.; Xue, B. Glutamic Acid Adsorption and Transformations on Silica. *J. Phys. Chem. C* **2011**, *115* (44), 21813–21825.

(12) Lambert, J.-F.; Jaber, M.; Georgelin, T.; Stievano, L. A Comparative Study of the Catalysis of Peptide Bond Formation by Oxide Surfaces. *Phys. Chem. Chem. Phys.* **2013**, *15* (32), 13371–10.

(13) Martra, G.; Deiana, C.; Sakhno, Y.; Barberis, L.; Fabbiani, M.; Pazzi, M.; Vincenti, M. The Formation and Self-Assembly of Long Prebiotic Oligomers Produced by the Condensation of Unactivated Amino Acids on Oxide Surfaces. *Angew. Chem., Int. Ed.* **2014**, *53* (18), 4671–4674.

(14) Lambert, J.-F.; Stievano, L.; Lopes, I.; Gharsallah, M.; Piao, L. The Fate of Amino Acids Adsorbed on Mineral Matter. *Planet. Space Sci.* **2009**, *57* (4), 460–467.

(15) Comerford, J. W.; Clark, J. H.; Macquarrie, D. J.; Breeden, S. W. Clean, Reusable and Low Cost Heterogeneous Catalyst for Amide Synthesis. *Chem. Commun.* **2009**, *8* (18), 2562–2563.

(16) Bujdák, J.; Rode, B. M. The Effect of Smectite Composition on the Catalysis of Peptide Bond Formation. *J. Mol. Evol.* **1996**, *43* (4), 326–333.

(17) Bujdák, J.; Rode, B. M. Glycine Oligomerization on Silica and Alumina. *React. Kinet. Catal. Lett.* **1997**, *62* (2), 281–286.

(18) Rodriguez-Garcia, M.; Surman, A. J.; Cooper, G. J. T.; Suarez-Marina, I.; Hosni, Z.; Lee, M. P.; Cronin, L. Formation of Oligopeptides in High Yield Under Simple Programmable Conditions. *Nat. Commun.* **2015**, *6*, 8385.

(19) Schaefer, D. W.; Keefer, K. D. Structure of Random Porous Materials: Silica Aerogel. *Phys. Rev. Lett.* **1986**, *56* (20), 2199–2202.

(20) Tarn, D.; Ashley, C. E.; Xue, M.; Carnes, E. C.; Zink, J. I.; Brinker, C. J. Mesoporous Silica Nanoparticle Nanocarriers: Biofunctionality and Biocompatibility. *Acc. Chem. Res.* **2013**, *46* (3), 792–801.

(21) Maleki, H.; Durães, L.; García-González, C. A.; del Gaudio, P.; Portugal, A.; Mahmoudi, M. Synthesis and Biomedical Applications of Aerogels: Possibilities and Challenges. *Adv. Colloid Interface Sci.* **2016**, *236*, 1–27.

(22) Schaefer, D. W.; Hurd, A. J. Growth and Structure of Combustion Aerosols: Fumed Silica. *Aerosol Sci. Technol.* **1990**, *12* (4), 876–890.

(23) Tang, F.; Li, L.; Chen, D. Mesoporous Silica Nanoparticles: Synthesis, Biocompatibility and Drug Delivery. *Adv. Mater.* **2012**, *24* (12), 1504–1534.

(24) Rahman, I. A.; Padavettan, V. Synthesis of Silica Nanoparticles by Sol-Gel: Size-Dependent Properties, Surface Modification, and Applications in Silica-Polymer Nanocomposites - a Review. *J. Nanomater.* **2012**, *2012* (30), 132424.

(25) Liu, C. C.; Maciel, G. E. The Fumed Silica Surface: a Study by NMR. *J. Am. Chem. Soc.* **1996**, *118* (21), 5103–5119.

(26) Wu, S.; Mou, C.; Lin, H. Synthesis of Mesoporous Silica Nanoparticles. *Chem. Soc. Rev.* **2013**, *42* (9), 3862–3875.

(27) Li, Z.; Barnes, J. C.; Bosoy, A.; Stoddart, J. F.; Zink, J. I. Mesoporous Silica Nanoparticles in Biomedical Applications. *Chem. Soc. Rev.* **2012**, *41* (7), 2590–2605.

(28) Gao, Q.; Xu, W.; Xu, Y.; Wu, D.; Sun, Y.; Deng, F.; Shen, W. Amino Acid Adsorption on Mesoporous Materials: Influence of Types of Amino Acids, Modification of Mesoporous Materials, and Solution Conditions. *J. Phys. Chem. B* **2008**, *112* (7), 2261–2267.

(29) Guo, C.; Holland, G. P. Investigating Lysine Adsorption on Fumed Silica Nanoparticles. *J. Phys. Chem. C* **2014**, *118* (44), 25792–25801.

(30) Rimola, A.; Sodupe, M.; Ugliengo, P. Affinity Scale for the Interaction of Amino Acids with Silica Surfaces. *J. Phys. Chem. C* **2009**, *113* (14), 5741–5750.

- (31) Ben Shir, I.; Kababya, S.; Schmidt, A. Molecular Details of Amorphous Silica Surfaces Determine Binding Specificity to Small Amino Acids. *J. Phys. Chem. C* **2014**, *118* (15), 7901–7909.
- (32) Guo, C.; Holland, G. P. Alanine Adsorption and Thermal Condensation at the Interface of Fumed Silica Nanoparticles: a Solid-State NMR Investigation. *J. Phys. Chem. C* **2015**, *119* (45), 25663–25672.
- (33) Ben Shir, I.; Kababya, S.; Schmidt, A. Binding Specificity of Amino Acids to Amorphous Silica Surfaces: Solid-State NMR of Glycine on SBA-15. *J. Phys. Chem. C* **2012**, *116* (17), 9691–9702.
- (34) Amitay-Rosen, T.; Kababya, S.; Vega, S. A Dynamic Magic Angle Spinning NMR Study of the Local Mobility of Alanine in an Aqueous Environment at the Inner Surface of Mesoporous Materials. *J. Phys. Chem. B* **2009**, *113* (18), 6267–6282.
- (35) Guo, C.; Holland, G. P.; Yarger, J. L. Lysine-Capped Silica Nanoparticles: a Solid-State NMR Spectroscopy Study. *MRS Adv.* **2016**, *1* (31), 2261–2266.
- (36) Folliet, N.; Gervais, C.; Costa, D.; Laurent, G.; Babonneau, F.; Stievano, L.; Lambert, J.-F.; Tielens, F. A Molecular Picture of the Adsorption of Glycine in Mesoporous Silica Through NMR Experiments Combined with DFT-D Calculations. *J. Phys. Chem. C* **2013**, *117* (8), 4104–4114.
- (37) Lopes, I.; Piao, L.; Stievano, L.; Lambert, J.-F. Adsorption of Amino Acids on Oxide Supports: a Solid-State NMR Study of Glycine Adsorption on Silica and Alumina. *J. Phys. Chem. C* **2009**, *113* (42), 18163–18172.
- (38) Burneau, A.; Barres, O.; Gallas, J. P.; Lavalley, J. C. Comparative Study of the Surface Hydroxyl Groups of Fumed and Precipitated Silicas. *Langmuir* **1990**, *6*, 1364–1372.
- (39) Morrow, B. A.; McFarlan, A. J. Surface Vibrational Modes of Silanol Groups on Silica. *J. Phys. Chem.* **1992**, *96*, 1395–1400.
- (40) Brei, V. V. ^{29}Si Solid-State NMR Study of the Surface Structure of Aerosil Silica. *J. Chem. Soc., Faraday Trans.* **1994**, *90* (19), 2961–2964.
- (41) Gun'ko, V. M.; Voronin, E. F.; Pakhlov, E. M.; Zarko, V. I.; Turov, V. V.; Guzenko, N. V.; Leboda, R.; Chibowski, E. Features of Fumed Silica Coverage with Silanes Having Three or Two Groups Reacting with the Surface. *Colloids Surf., A* **2000**, *166*, 187–201.
- (42) Aboshi, A.; Kurumoto, N.; Yamada, T.; Uchino, T. Influence of Thermal Treatments on the Photoluminescence Characteristics of Nanometer-Sized Amorphous Silica Particles. *J. Phys. Chem. C* **2007**, *111* (24), 8483–8488.
- (43) Peng, L.; Qisui, W.; Xi, L.; Chaocan, Z. Investigation of the States of Water and OH Groups on the Surface of Silica. *Colloids Surf., A* **2009**, *334* (1–3), 112–115.
- (44) Bakaev, V. A.; Pantano, C. G. Inverse Reaction Chromatography. 2. Hydrogen/Deuterium Exchange with Silanol Groups on the Surface of Fumed Silica. *J. Phys. Chem. C* **2009**, *113* (31), 13894–13898.
- (45) Vaccaro, G.; Agnello, S.; Buscarino, G.; Gelardi, F. M. Thermally Induced Structural Modification of Silica Nanoparticles Investigated by Raman and Infrared Absorption Spectroscopies. *J. Phys. Chem. C* **2010**, *114* (33), 13991–13997.
- (46) Zhang, H.; Dunphy, D. R.; Jiang, X.; Meng, H.; Sun, B.; Tarn, D.; Xue, M.; Wang, X.; Lin, S.; Ji, Z.; Li, R.; Garcia, F. L.; Yang, J.; Kirk, M. L.; Xia, T.; Zink, J. I.; Nel, A.; Brinker, C. J. Processing Pathway Dependence of Amorphous Silica Nanoparticle Toxicity: Colloidal vs Pyrolytic. *J. Am. Chem. Soc.* **2012**, *134* (38), 15790–15804.
- (47) Pavan, C.; Fubini, B. Unveiling the Variability of “Quartz Hazard” in Light of Recent Toxicological Findings. *Chem. Res. Toxicol.* **2017**, *30* (1), 469–485.
- (48) Stöber, W.; Fink, A.; Bohn, E. Controlled Growth of Monodisperse Silica Spheres in the Micron Size Range. *J. Colloid Interface Sci.* **1968**, *26* (1), 62–69.
- (49) Bennett, A. E.; Rienstra, C. M.; Auger, M.; Lakshmi, K. V.; Griffin, R. G. Heteronuclear Decoupling in Rotating Solids. *J. Chem. Phys.* **1995**, *103* (16), 6951–6958.
- (50) Hayashi, S.; Hayamizu, K. Chemical Shift Standards in High-Resolution Solid-State NMR (1) ^{13}C , ^{29}Si , and ^1H Nuclei. *Bull. Chem. Soc. Jpn.* **1991**, *64* (2), 685–687.
- (51) Hayashi, S.; Hayamizu, K. Chemical Shift Standards in High-Resolution Solid-State NMR (2) ^{15}N Nuclei. *Bull. Chem. Soc. Jpn.* **1991**, *64* (2), 688–690.
- (52) Iler, R. K. *The Chemistry of Silica*; Wiley and Sons, 1979.
- (53) Bhate, M. P.; Woodard, J. C.; Mehta, M. A. Solvation and Hydrogen Bonding in Alanine- and Glycine-Containing Dipeptides Probed Using Solution- and Solid-State NMR Spectroscopy. *J. Am. Chem. Soc.* **2009**, *131* (27), 9579–9589.
- (54) Jenkins, J. E.; Creager, M. S.; Butler, E. B.; Lewis, R. V.; Yarger, J. L.; Holland, G. P. Solid-State NMR Evidence for Elastin-Like B-Turn Structure in Spider Dragline Silk. *Chem. Commun.* **2010**, *46* (36), 6714–3.
- (55) Garcia, A. R.; de Barros, R. B.; Lourenço, J. P.; Ilharco, L. M. The Infrared Spectrum of Solid L-Alanine: Influence of pH-Induced Structural Changes. *J. Phys. Chem. A* **2008**, *112* (36), 8280–8287.
- (56) Barth, A. Infrared Spectroscopy of Proteins. *Biochim. Biophys. Acta, Bioenerg.* **2007**, *1767* (9), 1073–1101.
- (57) Brack, A. From Interstellar Amino Acids to Prebiotic Catalytic Peptides: a Review. *Chem. Biodiversity* **2007**, *4* (4), 665–679.
- (58) Hemley, R.; Mao, H.; Bell, P.; Mysen, B. Raman Spectroscopy of SiO_2 Glass at High Pressure. *Phys. Rev. Lett.* **1986**, *57* (6), 747–750.
- (59) Goller, D. D.; Phillips, R. T.; Sayce, I. G. Structural Relaxation of SiO_2 At Elevated Temperatures Monitored by *In Situ* Raman Scattering. *J. Non-Cryst. Solids* **2009**, *355* (34–36), 1747–1754.
- (60) Rimola, A.; Sodupe, M.; Ugliengo, P. Amide and Peptide Bond Formation: Interplay Between Strained Ring Defects and Silanol Groups at Amorphous Silica Surfaces. *J. Phys. Chem. C* **2016**, *120* (43), 24817–24826.